Study of the multiple melting behaviour of the aromatic polyimide LaRC CPI-2

Don K. Brandom and Garth L. Wilkes*

Department of Chemical Engineering, Polymer Materials and Interfaces Laboratory, Virginia Polytechnic Institute and State University, Blacksburg, VA 24061, USA

(Received 3 February 1994; revised 11 May 1994)

The dual melting behaviour of a rigid aromatic polyimide synthesized from 1,4-bis(4-aminophenoxy-4'-benzoyl)benzene and oxydiphthalic dianhydride was analysed. Film samples were synthesized through a stepwise imidization procedure wherein molecular weight control was effected through stoichiometric offset. The films display a glass transition temperature of 217°C and dual endothermic transitions at ca. 334°C and 364°C. Transmission electron microscopy, wide angle X-ray diffraction and small angle X-ray scattering (SAXS) studies, in conjunction with dynamic scanning calorimetry (d.s.c.) analysis, show that the higher melting transition results from the melting of lamellae which were melt recrystallized during heating in the d.s.c. D.s.c. heating rate studies reveal that the rate of transformation from thin to thick lamellae is dependent upon molecular weight, as expected. Synchrotron SAXS analysis confirms that the melt recrystallization process is very rapid for this high glass transition, low molecular weight polymer.

(Keywords: multiple melting; melt recrystallization; dynamic scanning calorimetry)

INTRODUCTION

Since the 1970s, there has been considerable effort placed on achieving high temperature thermally stable polymeric materials for use in structural applications. One of the prime materials that has been developed is the polyimide class of polymers, the majority of which are amorphous. The limitation, with respect to stiffness, of such systems is that the glass transition temperature is the variable governing the upper use temperature. Furthermore, while many of these amorphous systems are thermally stable (glass transition temperatures of 300–400°C), they often display poor solvent resistance–a material response that is unacceptable in many applications.

Since crystallinity tends to promote enhanced solvent resistance as well as provide a higher temperature stiffness, there has been a considerable thrust of research aimed at developing semicrystalline polyimide systems. Strong contributions to this area have come from the workers at the NASA–Langley Research Center[1-7] and have led to a variety of crystallizable polyimide materials. Some of these materials have been investigated for their general structural characteristics as either adhesives or matrix resins for high temperature composites. One of the crystallizable polyimides developed recently by researchers at NASA–Langley is LaRC CPI-2 ($M_w = 759\,g\,mol^{-1}$) (Langley Research Center Crystalline Polyimide, second generation), the structure of which is:

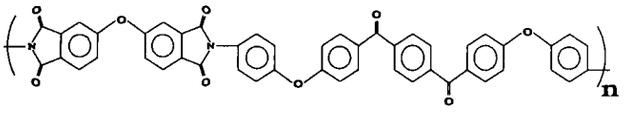

The glass transition temperature of this rigid aromatic polyimide is ca. 217°C. Low molecular weight samples of this polymer display dual endothermic transitions at ca. 334°C and 364°C during dynamic scanning calorimetry (d.s.c.) analysis (see *Figure 1*). This dual endothermic response is evident on both the first and second heating scans (followed by a $10°C\,min^{-1}$ cooling to the glass), though the overall magnitude of each transition is reduced upon reheating. It is important to understand the origins of this dual endothermic response from the perspective that a higher-melting polymer is more desirable owing to its potential use in high temperature applications. This paper presents results of an investigation into the morphological origins of this dual melting

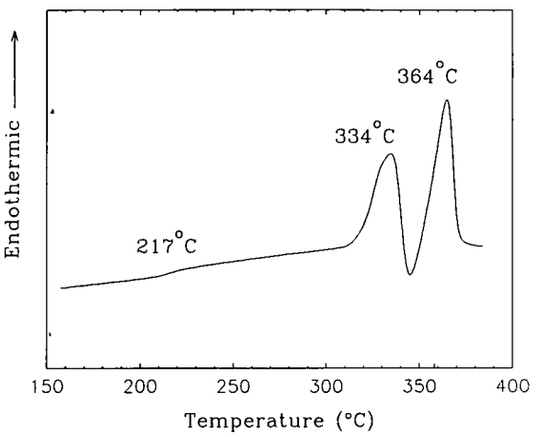

Figure 1 D.s.c. scan of a low molecular weight LaRC CPI-2 film displaying a glass transition temperature of ca. 217°C and two endothermic transitions at 334°C and 364°C

* To whom correspondence should be addressed

0032-3861/94/26/5672-06

phenomenon and provides evidence for a rapid lamellar melt recrystallization process.

The presence of a dual endothermic response during d.s.c. analysis has been noted in a number of other polymers. Keller *et al.*[8] found that by annealing polyethylene crystals at 128.5°C (from the melt) two distinct melting transitions developed at times between 2 and 100 min. The first transition temperature of 131°C remained constant with annealing time. However, the second transition ranged from 134°C to 136°C, the temperature being higher with longer crystallization times. The relative proportion of the overall crystallinity contribution by the higher melting transition increased with annealing time in a logarithmic fashion. For times less than 2 min only the 131°C peak was noted and for times longer than 100 min only the 136°C peak existed. Electron microscopy of a sample annealed so as to present a dual melting response revealed a dual population of thick and thin lamellae. The authors' conclusion that the dual melting response corresponded to the melting of thick and thin lamellae (produced through an isothermal lamellar thickening process) was thus well supported. In a crystallization study of ultralong n-paraffins Ungar *et al.*[9] found a dual melting response develop as a result of once-folded lamellar crystals melting and reorganizing into extended chain (higher-melting) crystals. In a study of low molecular weight poly(ethylene oxide) (PEO) crystals, Cheng *et al.*[10] assigned multiple endothermic and exothermic events to consecutive melting and recrystallization events, respectively, which yielded successively higher-melting, more extended chain crystals. Similarly, in studies of nylon-6,6 and polyethylene terephthalate[11,12] it has been determined that a melt reorganization/lamellar thickening process is occurring during heating to give rise to a second (higher) melting transition. In a crystallization study of an aromatic polyketone, Blundell *et al.*[13] found a coupled melting and recrystallization process occurring at about 260°C. The highest melting transition was attributed to the melting of melt-recrystallized 'thicker' lamellae. As an explanation for the presence of the dual endothermic transition, the authors propose that there is a kinetic barrier to be overcome in order to form thicker lamellae. Specifically, the *meta* linkages at the ends of the repeat units prohibit a continuous lamellar thickening process since the energy required for their incorporation requires that the thinner lamellae must first melt before reorganization can take place. Cheng and coworkers[14,15] found that in a polyimide system based on an oxydiphthalic dianhydride (OPDA)–poly(ethylene oxide) (PEO) copolymer ($n=3$ OPDA), high-melting crystals formed initially with subsequent formation of lower-melting crystals with time during isothermal crystallization. The lower endotherm in the ODPA–PEO polyimide was attributed to the melting of thinner-branched or in-filled lamellar structures[15].

This paper will introduce morphological and thermal analytical evidence for a relatively rapid lamellar melt reorganization process in LaRC CPI-2. The highest melting transition observed is the result of the melting of 'thick' lamellae formed from the melting and recrystallization of thinner lamellae during heating in a d.s.c.

Table 1 Calculated number average repeat unit length and molecular weight values based on the Carothers relationship

Stoichiometric offset (%)	$\langle X_n \rangle$	$10^{-3}\langle M_n \rangle$ (g mol^{-1})
0	∞	∞
2.5	79	30
5.0	39	15
7.5	26	9.8
10.0	19	7.2

EXPERIMENTAL

Synthesis

The synthetic process used for the production of the LaRC CPI-2 polyimide films was developed by researchers at NASA–Langley[4–7]. 1,4-Bis(4-aminophenoxy-4′-benzoyl)benzene (1,4-BABB) was reacted with oxydiphthalic dianhydride (ODPA) and phthalic anhydride (PA) to form a phthalic anhydride end-capped poly(amic acid) at a solids concentration of 15% (w/w) in dimethyl acetamide (DMAc) or *N*-methylpyrrolidinone (NMP). The reactions proceeded under a nitrogen blanket, at room temperature with stirring, for approximately 18 h. The poly(amic acid) was then removed and centrifuged for approximately 1 h and then cast onto a clean, dry glass plate and spread out with a doctor-blade set at a 30 mil gap (1 mil = 0.0254 mm). The films were dried under forced dry air overnight until non-tacky to the touch. Imidization was achieved by placing the films in a forced air oven for 1 h each at 50°C, 100°C, 200°C and 300°C. The oven was then allowed to cool slowly to room temperature. Films were removed from the glass by soaking in ca. 50°C water. A series of LaRC CPI-2 polyimide films were synthesized in order to provide a range of sample molecular weights. Molecular weight control was promoted through stoichiometric offset of the monomers. The predicted number average repeat unit length and molecular weight values calculated from the Carothers[16] relationship are given in *Table 1*.

Characterization

Dynamic scanning calorimetry (d.s.c.) was performed on a Seiko model 210 under a nitrogen purge of 20 ml min^{-1} at a heating rate of 20°C min^{-1}, unless otherwise noted. Wide angle X-ray diffraction (WAXD) was performed on a Nicolet model Stoe/V-2000 X-ray diffractometer using CuKα radiation with a wavelength of 1.54 Å. Values of 2θ from 3° to 40° were scanned at 0.05° steps with a 10 s dwell. Smeared small angle X-ray scattering (SAXS) profiles were taken from a slit-collimated compact Kratky equipped with a M. Braun position sensitive detector. The X-ray source was a Philips PW-1729 generator providing Ni-filtered CuKα radiation with a wavelength of 1.54 Å. Real-time SAXS measurements were carried out on the SUNY X3A2 beamline at the National Synchrotron Light Source (NSLS) at the Brookhaven National Laboratory ($\lambda = 1.54$ Å). Data were collected using a linear position sensitive detector (EG&G, PARC, model 1453) in the angular range $2\theta = 0$–1.5°. Pinhole SAXS data were collected using modified Kratky optics (with a sample to detector distance of 495 mm and a beam size of 1.5 × 0.2 mm). For the temperature jump experiment the sample was equilibrated in an external chamber at 300°C and then moved to the sample chamber set at 331°C by means of a

pneumatic piston. The estimated equilibration time at the higher temperature was approximately 20 s. Microtome film samples for transmission electron microscopy (TEM) were prepared from epoxy-embedded samples on a Reichert–Jung Ultracut E43 equipped with a diamond knife. No staining of the films was necessary since the lamellar textures were readily visible without a staining agent, as reported earlier for the similar LaRC CPI-1 system[17]. In fact, attempts at staining these particular polyimides with osmium tetraoxide or ruthenium tetroxide resulted in an obliteration of the otherwise visible lamellae[18]. TEM work was performed on a Philips model 1L 420T STEM.

RESULTS AND DISCUSSION

The calorimetric analysis of the films listed in *Table 1* reveals a distinct dependence of the crystallinity upon molecular weight. As seen from the d.s.c. scans in *Figure 2*, the semicrystalline character increases with increasing stoichiometric offset (lower M_n) in the untreated films. Furthermore, the dual melting transitions at ca. 334°C and 364°C become evident at 5.0% stoichiometric offset and are more pronounced for the higher offset films. The

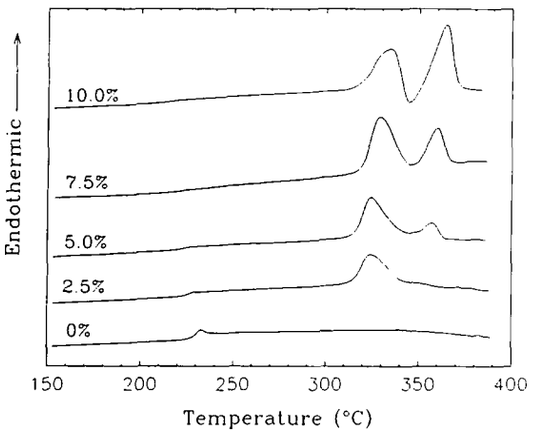

Figure 2 D.s.c. thermograms of stoichiometrically offset LaRC CPI-2 polyimide films showing the development of crystallinity with decreasing molecular weight

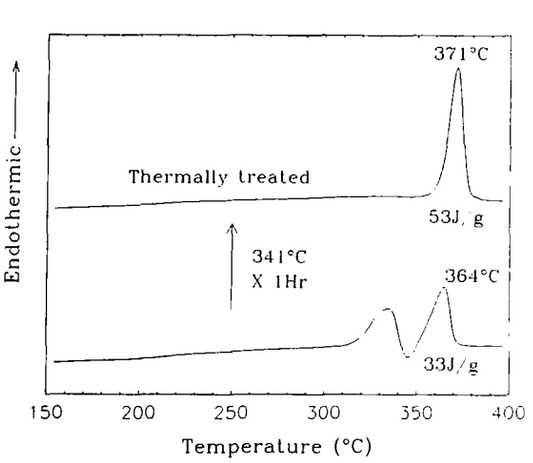

Figure 3 D.s.c. traces of an untreated and a 341°C-annealed 10.0% offset LaRC CPI-2 film showing the increase in heat of fusion and melting temperature with annealing

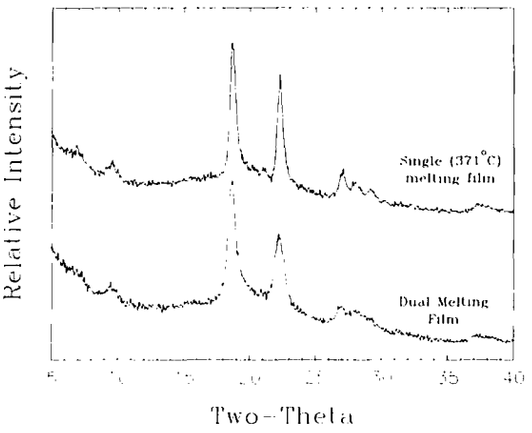

Figure 4 Wide angle X-ray diffraction scans for 10.0% offset LaRC CPI-2 films possessing dual and single (higher) melting transitions indicating the same crystal structure in both samples

exothermic peak between the two endotherms in the d.s.c. trace for the 10.0% stoichiometric offset film suggests that some crystallization process is occurring during the d.s.c. scan. The increase in the melting point for the first transition with decreasing molecular weight is most probably a kinetic result, as will be addressed below.

In order to isolate the crystal structure responsible for the higher melting peak from that responsible for the lower, a 10.0% offset film was annealed so as to possess only the higher melting transition. This was achieved by holding the film at a temperature of 341°C (near the maximum exotherm between the two endotherms) for 1 h (see *Figure 3*). The 341°C-annealed sample displayed a melting temperature, T_m, and heat of fusion value, ΔH_f, considerably higher than possessed by the second endotherm of an untreated sample: 371°C *versus* 364°C and 53 J g^{-1} *versus* ca. 33 J g^{-1}, respectively. In order to increase the population of the crystalline structures responsible for the lower melting transition (for subsequent analysis), a sample of the 10.0% offset film was annealed at 275°C for approximately 50 h. The result of this annealing was an increase in the magnitude of the lower melting entotherm. The ratio of the area under the first endotherm to that under the second in this sample was 2.3, more than double the value of 0.9 displayed by the as-made film. A slight change in the melting profiles shifted the melting temperatures only a small amount from 334°C and 364°C to 339°C and 361°C. WAXD analysis on portions of the 371°C-melting film and this 275°C-annealed sample revealed that there was no change in the crystal lattice structure as a result of the annealing process to form the high-melting structure: the diffraction profiles for both samples were identical with regard to the location of the diffraction peaks (see *Figure 4*). The better peak resolution seen for the 341°C-annealed film indicates a greater degree of crystalline order and/or greater crystallite size. *Figure 5* shows the SAXS profiles of these same films plotted as the smeared intensity as a function of s, where $s = 2/\lambda \sin\theta_B$, λ is the wavelength and θ_B is the Bragg angle. Here it can be seen that the smeared 'long spacing' increases from 180 Å in the 275°C-annealed sample to 230 Å in the 341°C-annealed sample. It should be noted here that desmearing and the Lorentz correction were not employed because only general trends in long spacing were sought.

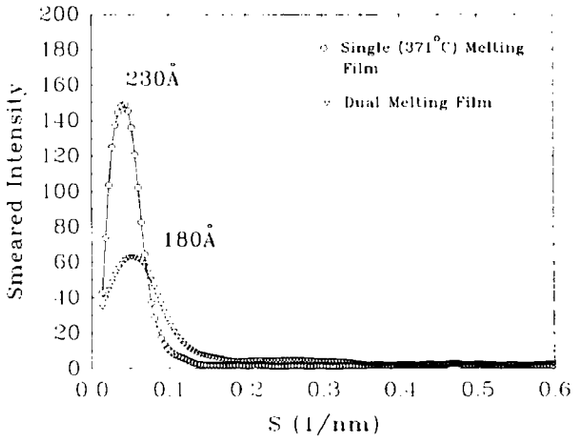

Figure 5 Smeared small angle X-ray scattering profiles for 10.0% offset LaRC CPI-2 films possessing dual and single (higher) melting transitions showing an increase in long spacing for the higher-melting film

All the evidence presented thus far suggests that the lower endothermic transition seen in the d.s.c. trace comes from the melting of relatively thin lamellae, whereas the higher melting transition originates from the melting of thicker lamellae. The melting point of a polymer lamella, where the lateral dimension is very much greater than the thickness, is directly related to its thickness through the fundamental thermodynamic relationship[19]

$$T_m = T_m^\circ\left(1 - \frac{2\sigma_e}{l\Delta H_f}\right) \quad (1)$$

where T_m is the observed melting temperature, T_m° is the thermodynamic (equilibrium) melting temperature, σ_e is the chain fold surface energy, ΔH_f is the heat of fusion per mole of crystalline repeat units and l is the lamellar thickness. As equation (1) shows, as l becomes larger the observed melting temperature approaches the equilibrium value.

As further support for the existence of a lamellar thickening process, transmission electron microscopy (TEM) was employed to detect differences in lamellar texture between the dual-melting and single-melting (371°C) films. In order to obtain TEM specimens with reasonable clarity of lamellar structures, another sample of the 10.0% offset film was annealed at 275°C for 65 h. This sample displayed dual melting transitions at 335°C and 360°C with a first to second peak area ratio of 2.7. The micrograph of the film possessing both melting transitions, shown in *Figure 6a*, reveals the presence of some faint, wisp-like lamellae. In the higher-melting film, thicker and more clearly defined lamellae are readily seen throughout the sample (see *Figure 6b*). Rough approximations of lamellar thicknesses estimated from the micrographs are 70 Å and 130 Å for the low and high temperature annealed films, respectively.

At this point, then, it has been established that the dual melting response is a result of the melting of 'thin' and 'thick' lamellae. The question remains, however, as to whether or not any 'thick' lamellae are already present in the films prior to d.s.c. analysis. As noted earlier, the existence of an exotherm between the two endotherms indicates that some melt recrystallization process is occurring. Because of the time dependent nature of the

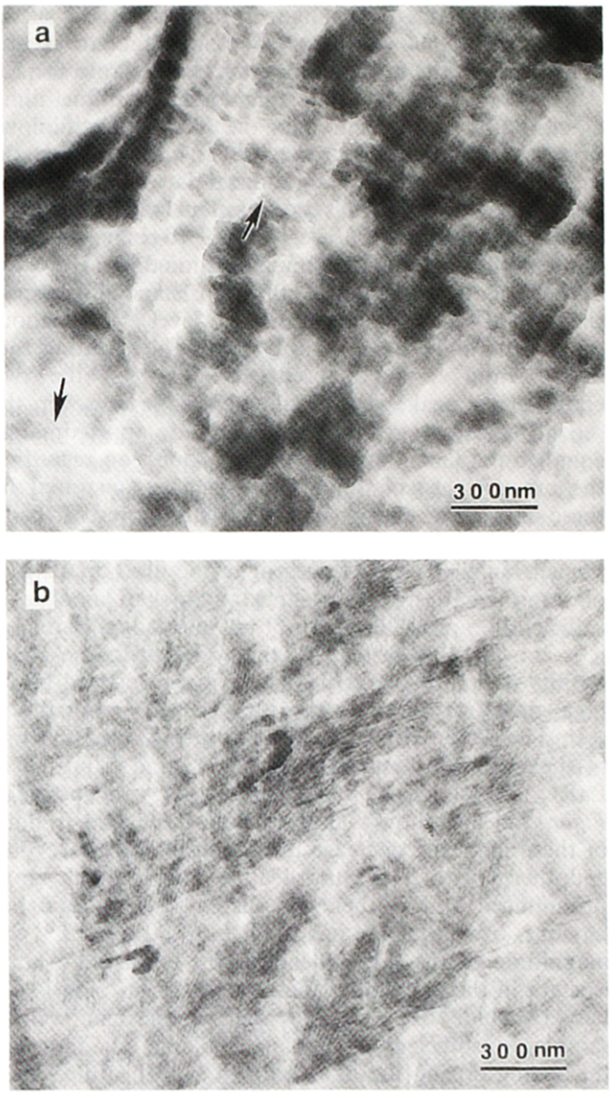

Figure 6 (a) TEM micrograph of the 10.0% offset LaRC CPI-2 film annealed to give a high population of the lower-melting structures. (b) TEM micrograph at the same magnification of another sample of the same film annealed to give a single endotherm at 371°C

recrystallization process, one would expect to see the magnitude of the second endotherm decrease, relative to the first, with higher d.s.c. heating rates because of a shorter available recrystallization time. An endotherm ratio analysis of the area under the first endotherm to that under the second as a function of heating rate was performed on the films presenting the dual melting response. The most consistent method for peak area integration was found to be the following: the first endotherm area integration limits were taken from the point at which the d.s.c. signal began to deviate from the baseline for the first endotherm to the signal minimum between the first and second endotherms. The second endotherm area integration limits were taken from the signal minimum to the point where the d.s.c. signal again returned to the baseline. This integration method is not meant to provide an exact measure of the true heat of melting. Rather, the objective is to uncover trends

regarding the relative changes in the magnitudes of the transitions. *Figure 7* displays a plot of first to second endotherm ratio as a function of heating rate for the 5.0%, 7.5% and 10.0% stoichiometric offset films. Focusing first on the curve for the 10.0% offset film, we note that at heating rates up to 30°C min^{-1} the magnitude of the second endotherm is seen to decrease relative to the first. This is consistent with a decrease in the conversion of lower-melting to higher-melting material through shorter recrystallization times. However, at the faster heating rates of 50°C min^{-1} and 70°C min^{-1} the first to second endotherm ratio levels out at about 1.1. At the highest (reasonably achievable) heating rate of 70°C min^{-1}, the elapsed time between the two endothermic peaks is approximately 25 s. However, the second transition remains in magnitude approximately equal to the first. Thus, the primary question regarding the pre-existence of 'thick' lamellae is unanswered by these data alone. Two possible scenarios present themselves. Either there is a small, but finite, population of thicker lamellae already present in the film, or the rate of transformation from thinner to thicker lamellae is sufficiently rapid that it cannot be detected by d.s.c., i.e. it is considerably faster than 25 s. Owing to the chain rigidity and stiffness of this polyimide, evidenced by its high glass transition temperature, the latter possibility seems unlikely. However, the endotherm ratio analysis of the higher molecular weight 7.5% and 5.0% offset LaRC CPI-2 films as a function heating rate shown in *Figure 7* clearly show that this is indeed the case. In both of these films the decrease in magnitude of the second endotherm with increasing heating rate is much more pronounced and neither film displays asymptotic behaviour. In fact, at the heating rate of 70°C min^{-1}, the magnitude of the second endotherm is virtually non-existent in the 5.0% offset film (about a 50:1 ratio). We may conclude that, for the higher molecular weight samples, insufficient time was available for lamellar thickening during the d.s.c. scan at high heating rates. By implication, then, there was sufficient time for transformation in the low molecular weight 10.0% offset film.

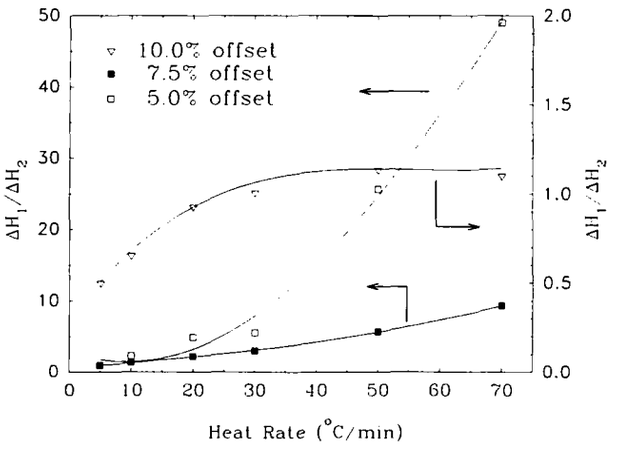

Figure 7 Ratio of the first to the second melting endotherm as a function of heating rate for the 5.0%, 7.5% and 10.0% offset LaRC CPI-2 films

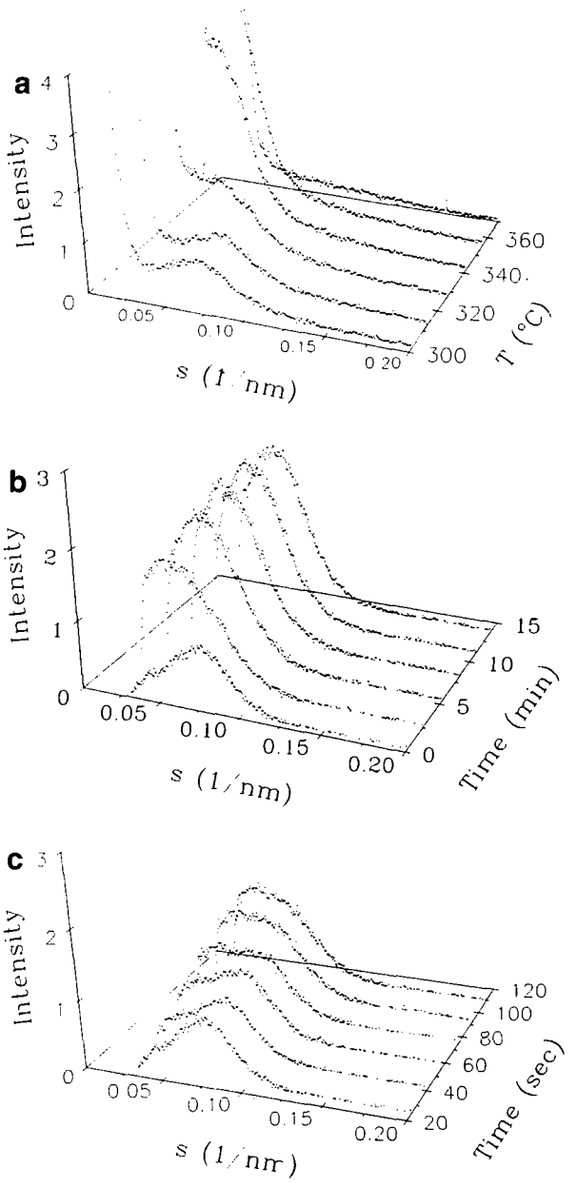

Figure 8 (a) Synchrotron SAXS scans of a 10.0% offset LaRC CPI-2 film as a function of temperature at a heating rate of 5°C min^{-1}. (b) Isothermal (331°C) scans of a different sample of the same film. (c) The first 2 min of the isothermal scans shown in (b). The upturn in intensity at low s values was removed from plots (b) and (c) for the sake of clarity

If we re-examine the d.s.c. traces displayed in *Figure 2*, it is apparent that the development of the dual endothermic response with decreasing molecular weight is a kinetic manifestation. That is, the lower molecular weight samples will have a lower melt viscosity and shorter reptation time and can recrystallize faster, thereby allowing for the presence of a second (higher) melting transition. The complete lack of a second endotherm in the 2.5% offset (high M_w) film, then, is also a kinetic result. In fact, at the slow heating rate of 5°C min^{-1}, a d.s.c. scan of this film reveals the presence of a second endotherm (not shown) that was otherwise masked by the 'fast' heating rate of 20°C min^{-1}. Thus, the conclusion to be drawn from the data thus far is that there are no 'thick' lamellae present in the films prior to d.s.c. analysis.

As indicated above, the rate of transformation of 'thin' to 'thick' lamellae in the 10.0% offset film occurred, with some surprise, very rapidly. In order to gain a real-time perspective of the rapid changes in lamellar dimensions as a result of thermal treatment of this sample, a SAXS analysis of the pinhole-collimated data from the NSLS was employed. Both a temperature ramp and temperature jump experiment were run with this material. In the ramping experiment the sample was heated from 300°C to 370°C at 5°C min^{-1}. *Figure 8a* shows a sample of the data collected during this run. The absolute intensity is plotted as a function of the angular variable *s*. A shift in the peak position to smaller *s* values (greater long spacings) is evident between 320°C and 350°C. As the film is taken through higher temperatures the lamellae melt and the SAXS peak disappears. The temperature jump experiment reveals the rapid development of the thicker lamellae under isothermal conditions. Here the sample was equilibrated at 300°C and then rapidly heated to 331°C and held for 15 min. The initial equilibration time at 331°C was approximately 20 s. From the peak positions shown in *Figure 8b* it is clear that nearly all of the changes have already occurred within the first 2.5 min. *Figure 8c* presents an expanded view of the changes occurring within the first 2 min. The development of the thicker lamellae is clearly seen to occur at the expense of the thinner lamellae within this short time-frame. It should be noted here that this 'annealing' temperature is about 10°C below that of the maximum in the exotherm between the two melting transitions. Hence, the rate of transformation is expected to be very much slower at this lower temperature. Given the time resolution restrictions (minimum of 17 s scans) of this experimental set-up, it is doubtful that the thickening phenomenon could be captured as clearly at 341°C.

CONCLUSIONS AND SUMMARY

Evidence presented in this paper regarding the dual melting transitions observed in LaRC CPI-2 polyimide films clearly points to a lamellar melt recrystallization process occurring during heating. A film sample annealed at the exotherm temperature between the two melting transitions displayed a higher melting transition with greater long spacing from SAXS and visibly thicker lamellae seen through transmission electron microscopy. This is entirely consistent with the fundamental thermodynamic relationships regarding crystal melting in polymeric systems. D.s.c. analysis indicates that the thickening process is a kinetic phenomenon dependent upon molecular weight. Furthermore, d.s.c. evidence suggests that only the lower-melting lamellae are present in the films initially. Despite the chain rigidity in this polyimide, d.s.c. and synchrotron SAXS analyses clearly show that the melt recrystallization process is very rapid for the 10.0% stoichiometric offset (lowest molecular weight) film. It is noteworthy that this melt reorganization process is occurring in polymer samples whose number average degrees of polymerization are rather low by polymer standards. The highest molecular weight sample displaying the melt reorganization process has a repeat unit length of 79, whereas the value for the lowest molecular weight film is only 19. An explanation for the exact mechanism of the melt reorganization process is not presently available. It is possible that a kinetic barrier exists to prevent a continuous lamellar thickening as has been suggested by Blundell *et al.*[13] for the poly(aryl ether ketone) in their study. Investigations are currently proceeding to help answer this question.

ACKNOWLEDGEMENTS

The authors appreciate the support of this research by the National Aeronautics and Space Administration under contract number NGT-51117. Also, the support of the National Science Foundation Science and Technology Center for High Performance Adhesives and Composites at Virginia Polytechnic under contract number DMR8809714 is greatly appreciated. We would also like to thank Paul Hergenrother, Dr Steven Havens and Heather Brink for their guidance regarding polyimide synthesis. Special thanks are due to Don Loveday for acquiring the synchrotron SAXS data and to Dr Ben Hsiao of DuPont for facilitating the use of this instrument and, along with Ravi Verma, for helpful discussions regarding synchrotron analysis. TEM work performed by Steve McCartney is sincerely appreciated.

REFERENCES

1 Bell, V. L., Stump, B. L. and Gager, H. *J. Polym. Sci.* 1976, **14**, 2275
2 Progar, D. J., Bell, V. L. and St Clair, T. L. *US Pat. 4065345* 1977
3 Bell, V. L. *US Pat. 4094862* 1978
4 Hergenrother, P. M., Wakelyn, N. T. and Havens, S. J. *J. Polym. Sci., Polym. Chem. Edn* 1987, **25**, 1093
5 Hergenrother, P. M. and Havens, S. J. *J. Polym. Sci., Polym. Chem. Edn* 1989, **27**, 1161
6 Hergenrother, P. M., Beltz, M. W. and Havens. S. J. *J. Polym. Sci., Polym. Chem. Edn* 1991, **29**, 1483
7 Havens, S. J. and Hergenrother, P. M. *J. Polym. Sci., Polym. Chem. Edn* 1992, **30**, 1209
8 Martinez-Salazar, J., Barham, P. J. and Keller, A. *J. Mater. Sci.* 1985, **20**, 1616
9 Ungar, G., Stejny, J., Keller, A., Bidd, I. and Whiting, M. C. *Science* 1985, **229**, 386
10 Cheng, S. Z. D., Zhang, A., Chen, J. and Heberer, D. P. *J. Polym. Sci., Polym. Phys. Edn* 1991, **19**, 287
11 Bell, J. P., Slade, P. E. and Dumbelton, J. H. *J. Polym. Sci. A-2* 1968, **6**, 1773
12 Bell, J. P. and Dumbelton, J. H. *J. Polym. Sci. A-2* 1969, **7**, 1033
13 Blundell, D. J., Liggat, J. J. and Flory, A. *Polymer* 1992, **33**, 2475
14 Cheng, S. Z. D., Heberer, D. P., Lien, H. and Harris, F. W. *J. Polym. Sci., Polym. Phys. Edn* 1990, **28**, 655
15 Heberer, D. P., Cheng, S. Z. D., Barley, J. S., Lien, H., Bryant, R. G. and Harris, F. W. *Macromolecules* 1991, **24**, 1890
16 Carothers, W. H. *J. Am. Chem. Soc.* 1929, **51**, 2548
17 Muellerleile, J. T., York, G. A. and Wilkes, G. L. *Polym. Commun.* 1991, **32**, 176
18 Muellerleile, J. T. personal communication
19 Hoffman, J. D. and Weeks, J. J. *J. Res. Natl Bur. Stand., Sect. A* 1962, **66**, 13